Structural and vibrational properties of {N,N} pairs and {N,H} complexes in Si

J. L. McAfee, He Ren, and S. K. Estreicher*
Physics Department, Texas Tech University, Lubbock, Texas 79409-1051, USA
(Received 4 June 2003; revised manuscript received 27 August 2003; published 19 April 2004)

First-principles molecular-dynamics simulations are used to predict the structures and binding energies of interstitial nitrogen N_i, substitutional nitrogen N_s, the N_i-self-interstitial complex, the $\{N_i,N_i\}$, $\{N_i,N_s\}=\{N_2,V\}$, and $\{N_s,N_s\}=\{N_2,V_2\}$ pairs (V is the vacancy). The interactions of N with H in Si are studied and the properties of several {N,H} complexes are predicted. The dynamical matrices yield many new local and pseudolocal vibrational modes associated with the impurities and their Si nearest neighbors. The unidentified {N,H}-related infrared absorption line reported by Pajot *et al.* is assigned to the $\{N_s,H\}$ complex.

DOI: 10.1103/PhysRevB.69.165206 PACS number(s): 61.72.Ji, 71.55.Cn

I. INTRODUCTION

Nitrogen impurities, first detected in 1959,[1] play many useful roles in Si. Despite its low equilibrium solubility,[2] N increases the mechanical strength of the crystal by locking dislocations,[3–5] suppresses the formation of D defects and improves oxide integrity,[6,7] interacts with O,[2,8,9] and affects O precipitation.[10,11] Nitrogen is also involved in the "*ABC*" photoluminescence band[12–14] caused by a trigonal isoelectronic defect involving N and possibly Al as well.

Substitutional nitrogen N_s was identified by electron paramagnetic resonance (EPR) as the SL5 center.[15,16] Isolated N_s is off-center along the trigonal axis, threefold coordinated, and over 70% of the odd electron resides on its fourth Si nearest neighbor. This center reorients at low temperature with an activation energy of 0.107 ± 0.02 eV (Ref. 16) and averages out to tetrahedral symmetry above 150 K.[17] The observed off-center structure of N_s was unexpected at the time and stimulated a number of theoretical studies.[18–24]

However, channeling studies[25,26] imply that over 95% of N is at interstitial rather than substitutional sites. Electrical and Hall effect measurements[27] show that less than 1% of the implanted N behaves like a donor. Using Fourier-transform infrared (FTIR) absorption, Stein[28–31] demonstrated that most of the implanted N in Si forms {N,N} pairs and only 1% or so becomes substitutional. The (^{14}N) pairs are characterized by two strong IR lines at 766 and 963 cm^{-1} (749 and 937 for ^{15}N, respectively, with new lines at 759 and 948 with mixed isotopes). The two N atoms in the pair are equivalent.[26] A weaker IR line[31] at 653 cm^{-1} correlates with the SL5 EPR center and is attributed to N_s.

Studies in Ge (Ref. 32) reveal the same centers as in Si, but for a new line at 590 cm^{-1} in Ge. It appears to be related to a weak 691 cm^{-1} line in Si. No identification of the associated defect was proposed. The 691 cm^{-1} line anneals out just as the N pair lines start to grow,[33] suggesting that it could be associated[34] with interstitial nitrogen N_i. This interstitial is predicted to be highly mobile,[35] migrating from one split-$\langle 100\rangle$ configuration to another through a puckered bond-centered site, with an activation energy of 0.5 eV.

The dominant nitrogen defect in Si was identified[26] as the interstitial-interstitial pair $\{N_i,N_i\}$, a square with two N's (and two Si's) at opposite corners. This configuration (which agrees with ours) is discussed below. Recent calculations[36] suggest that this pair diffuses with an activation energy of the order of 3 eV.

Nitrogen also interacts with the vacancy V.[37–39] Nitrogen-V interactions such as $N_s+V\rightarrow\{N_s,V\}$, $\{N_i,N_i\}+V\rightarrow\{N_i,N_s\}$ (also called $\{N_2,V\}$), or $\{N_i,N_i\}+V_2\rightarrow\{N_s,N_s\}$ (also called $\{N_2,V_2\}$) have been considered by several authors.[40–43] The $\{N_s,N_s\}$ complex is found to be particularly stable. In Ref. 41, the binding energies relative to $\{N_i,N_i\}$ and an isolated V or V_2 are 0.8 eV for $\{N_i,N_s\}$ and 3.6 eV for $\{N_s,N_s\}$. The recent theoretical study of Goss *et al.*[43] discusses N_i, the $\{N_i,N_i\}$ pair and its interaction with a self-interstitial or a vacancy, N_s, the $\{N_s,V\}$ complex, and the $\{N_s,N_s\}$ pair and its interactions with a vacancy.

H interacts with many defects and impurities in Si (Refs. 44 and 45) and is sometimes introduced into the crystal from a H-rich SiN_x surface layer.[46,47] A number of FTIR lines associated with {N,H} complexes in the bulk of Si have been reported.[48] Several of the 21 lines tabulated are associated with known defects, others are not identified, but a weak line at 2967 cm^{-1} (2197 with D substitution) is tentatively assigned to a {N,H} complex.

In the present paper, we calculate the structures and energetics of isolated N and N pairs in Si. All the local and pseudolocal vibrational modes (LVM's and pLVM's) associated with the impurities and their Si nearest neighbors (NN's) are calculated and a number of new modes are predicted. The pLVM's are strongly localized N-related modes located below the Γ phonon. Their localization can be quantified[49] using the eigenvectors of the dynamical matrix. We also calculate the configurations, binding energies, and complete vibrational spectra of the $\{N_i,H\}$ and $\{N_s,H\}$ pairs, and show that the $\{N_i,N_i,H\}$ complex is unlikely to form. Section II describes the methodology, Sec. III deals with isolated N defects (N_i, $N_i+V=N_s$, and $N_i+I=\{N_i,I\}$, where I is the self-interstitial), Sec. IV deals with nitrogen pairs

($\{N_i,N_i\}$, $\{N_i,N_i\}+V=\{N_i,N_s\}$, and $\{N_i,N_s\}+V=\{N_s,N_s\}$), and Sec. V contains our predictions for the $\{N_i,H\}$ and $\{N_s,H\}$ complexes. The key results, the formation energies, and a discussion are in Sec. VI. The Appendix contains tables of frequencies with isotopic substitutions (combinations of ^{15}N and/or D) for {N,N} pairs and {N,H} complexes.

II. THEORETICAL APPROACH

Our first-principles results are obtained from self-consistent molecular-dynamics (MD) simulations based on local-density-functional (DF) theory. The calculations are performed with the SIESTA code.[50,51] The exchange-correlation potential is that of Ceperley-Alder[52] as parametrized by Perdew-Zunger.[53] Norm-conserving pseudopotentials in the Kleinman-Bylander form[54] are used to remove the core regions from the calculations. The basis sets for the valence states are linear combinations of (numerical) atomic orbitals of the Sankey type[55,56] but generalized to be arbitrarily complete with the inclusion of multiple-ζ orbitals and polarization functions.[50] The charge density is projected on a real-space grid with equivalent cutoffs of 150 Ry to calculate the exchange-correlation and Hartree potentials. The host crystal is represented by a 64-host-atom periodic supercell.

The valence states are described with double-ζ (DZ) basis sets for N and H and double-ζ plus polarization (DZP) for Si (two sets of valence *s* and *p* plus one set of *d*'s). The cutoff radius for Si is just over 3 Å meaning that Si atoms farther than 6 Å do not overlap. In the perfect cell, a Si atom overlaps with 46 other Si atoms on five adjacent shells. The cutoff radii for N and H are over 2 Å. A $2\times2\times2$ Monkhorst-Pack[57] mesh is used for the *k*-point sampling. The dynamical matrices are calculated with $k=0$ using linear-response theory.[58] This allows the computation of the harmonic dynamical matrix of the cell from the derivatives of the density matrix relative to nuclear coordinates.

We calculated a number of small molecules containing N, Si, and/or H to test the basis sets and pseudopotentials. In these tests, the same cutoff radius was used as for the defect calculations. We find that a DZ basis is sufficient for H and N. A DZP basis is needed for Si unless it is close to a sp^2 (trigonal planar) or sp^3 (tetrahedral) hybridization. Our tests include the N_2 molecule, ammonia (NH_3), silane (SiH_4), and silylamine (H_3SiNH_2). The calculated (measured) quantities are as follows. For N_2, the N-N bond length is 1.124 Å (1.0975, Ref. 59) and the N-N stretch is 2392 cm^{-1} (2358, Ref. 60). For NH_3, the N-H bond length is 1.011 Å (1.008, Ref. 59) and the symmetric N-H stretch is 3461 cm^{-1} (3337, Ref. 60). For SiH_4, the Si-H bond length is 1.494 Å (1.474, Ref. 61), the triply degenerate antisymmetric Si-H stretch is 2252 cm^{-1} (2191, Ref. 60), and the symmetric Si-H stretch is 2180 cm^{-1} (2187, Ref. 60). Finally, in the case of H_3SiNH_2, we found no experimental structural details, but the calculated (measured[62]) modes are antisymmetric N-H stretch, 3592 cm^{-1} (3547), symmetric N-H stretch, 3479 cm^{-1} (3445), and symmetric Si-H stretch, 2181 cm^{-1} (2172). For the symmetric Si-N stretch we find a mode at 967 cm^{-1} which does not match its experimental identification of 845 cm^{-1}. The mode we find at 836 cm^{-1} is a Si-H_2 bend mode.

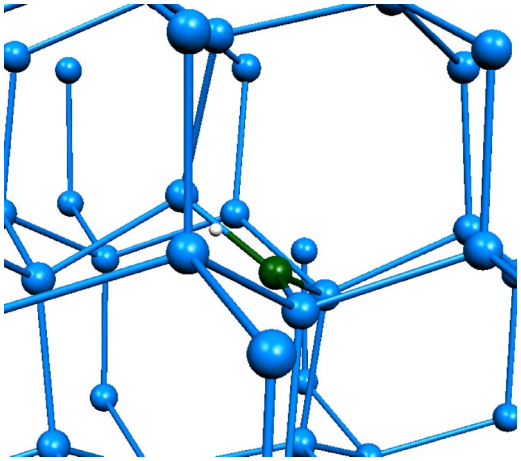

FIG. 1. (Color online) Fraction of the Si_{64} cell showing the N_i defect. The light gray (blue) spheres are Si atoms, the darker gray (green) sphere is N, and the small white ball shows the substitutional site.

III. ISOLATED NITROGEN

A. Interstitial nitrogen: N_i

The stable configuration of N_i was obtained by testing the tetrahedral and hexagonal interstitial sites, the (relaxed and puckered) bond-centered (BC) site N_{BC}, as well as the split-$\langle100\rangle$ and split-$\langle110\rangle$ configurations. The initial structures were all subjected to conjugate gradient optimizations until the maximum force component was less than 0.01 eV/Å.

The most stable energy structure (N_i, Fig. 1) is very close to a split-$\langle100\rangle$. Nitrogen binds to three Si atoms with almost identical N-Si bond lengths: 1.77, 1.78, and 1.79 Å, respectively. The small differences could be due to cell size effects. These bond lengths are just shorter than the sum of the covalent radii of N and Si (1.86 Å). The bond between N and the displaced Si atom makes a 15° angle toward $\langle110\rangle$ (13° has been reported by Goss *et al.*[43]). The three N-Si bond angles are 98°, 125°, and 137°. The symmetry is C_{1h}.

Of the other structures we tested, only N_{BC} is a local minimum of the energy, 0.48 eV higher than the configuration described above. This agrees well with 0.5 eV (Ref. 43) and 0.4 eV (Ref. 35) reported by other authors. Modeling studies[35,40] have suggested that N_i is a fast diffuser. Since the BC site is along the expected diffusion path[35] of N_i, the small energy difference we find between the two structures supports this conclusion.

The dynamical matrix yields the LVM's and pLVM's associated with N_i. The square of the relative amplitude A_{rel}^2 of the oscillation of the N atom is plotted as a function of the frequency in Fig. 2 (top). These amplitudes are normalized. Hence, in such a plot, a value close to 1.0 means that only

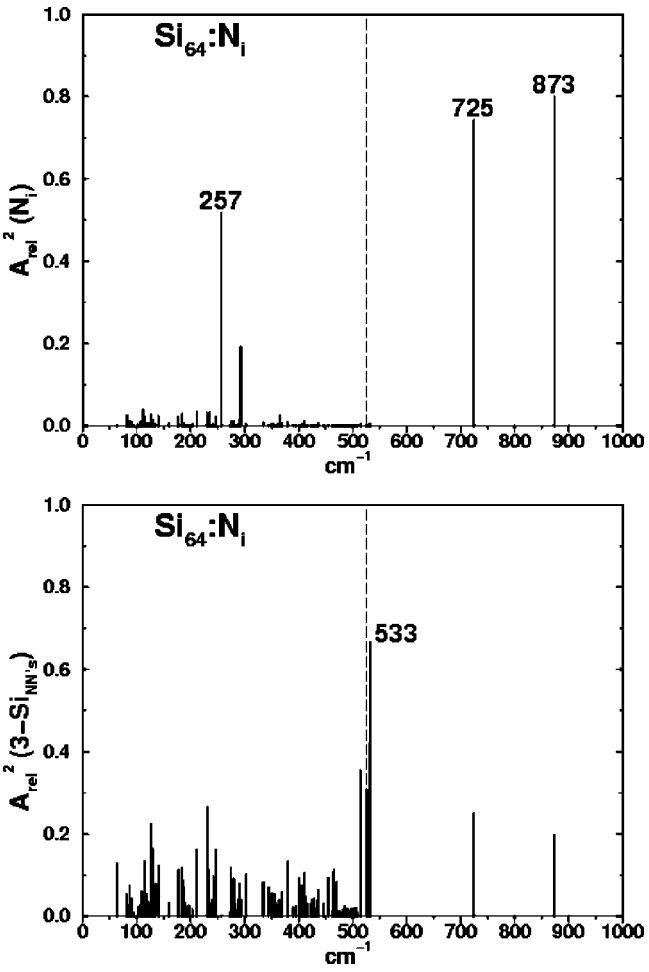

FIG. 2. Square amplitude of the oscillation of N_i (top) and of its three Si NNs (bottom) as a function of frequency (see text). The dashed line shows the calculated Γ phonon.

the N atom oscillates while all the Si atoms are mostly immobile. A value close to zero means that N remains still while other atoms in the cell oscillate. The square of the amplitude of the oscillation of the three Si NN's to N is plotted in Fig. 2 (bottom).

Four modes are associated with the N_i defect. Three of them involve substantial oscillations of N and the fourth involves the oscillation of its three Si NN's. The highest-lying mode, 873 cm^{-1}, is the symmetric N-Si stretch. The second-highest mode, 725 cm^{-1}, is the antisymmetric N-Si stretch.

TABLE I. Vibrational frequencies (cm^{-1}) associated with $^{14}N_i$ ($^{15}N_i$) in Si. The mode at 533 cm^{-1} does not involve the motion of the N atom.

C_{1h}	This work	Goss *et al.*[a]
A'	873 (850)	885 (862)
A'	725 (707)	773 (754)
A''	533 (533)	550 (550)
A''	257 (252)	

[a]Reference 43.

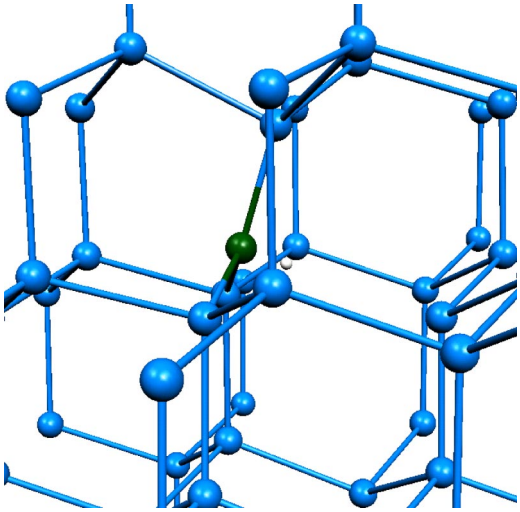

FIG. 3. (Color online) Fraction of the Si_{64} cell containing N_s. The light gray (blue) spheres are Si atoms, the darker gray (green) sphere is N, and the small white ball shows the substitutional site.

The N-Si wag is buried in the phonon band at 257 cm^{-1}, but still shows a substantial degree of localization. The fourth localized mode, a breathing mode of the three Si NN's to N_i at 533 cm^{-1}, is nearly resonant with the Γ phonon. Due to the low symmetry of this defect, C_{1h}, all of these modes are infrared (IR) active.

No experimental frequencies have been positively assigned to N_i. However, an IR line at 691 cm^{-1} has been tentatively assigned[2,32] to it. If this assignment is correct, the 691 cm^{-1} line corresponds to our 725 cm^{-1} line. Table I compares our frequencies to those calculated in Ref. 43.

B. Substitutional nitrogen: N_s

The reaction of N_i with a *preexisting* vacancy leads to the formation of N_s at a gain of 3.55 eV. This is less than the formation energy of the vacancy, $\sim$4 eV.[63] Thus, N_i should not spontaneously displace a host atom to become N_s. The equilibrium configuration of N_s is shown in Fig. 3.

It is known from EPR data[15,16] and numerous calculations[21–23,26,64] that N_s has C_{3v} symmetry, and our calculations confirm this. N is displaced from the perfect substitutional site by 0.73 Å along the trigonal axis. The three equivalent N-Si bonds are 1.85 Å and the sum

TABLE II. Vibrational frequencies (cm^{-1}) associated with $^{14}N_i$ ($^{15}N_i$) in Si.

C_3v	This work	Goss *et al.*[a]	Expt.[b]
E	664 (647)	637 (621)	653 (642)
A_1	222 (220)		

[a]Reference 43.
[b]Reference 2.

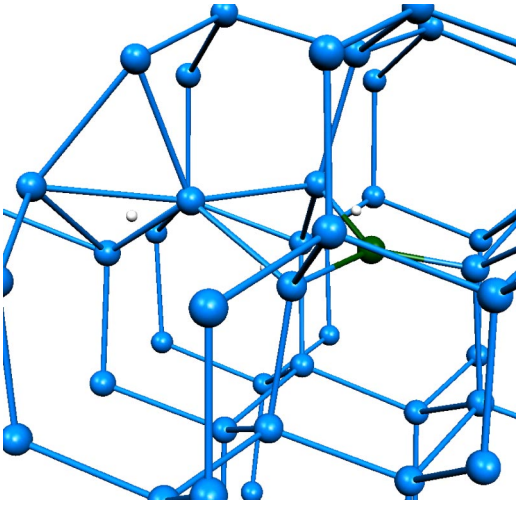

FIG. 4. (Color online) Fraction of the Si_{64} atom cell showing the $\{N_i,I\}$ complex. The light gray (blue) spheres are Si atoms, the darker gray sphere (green) is N, and the small white balls show the substitutional sites.

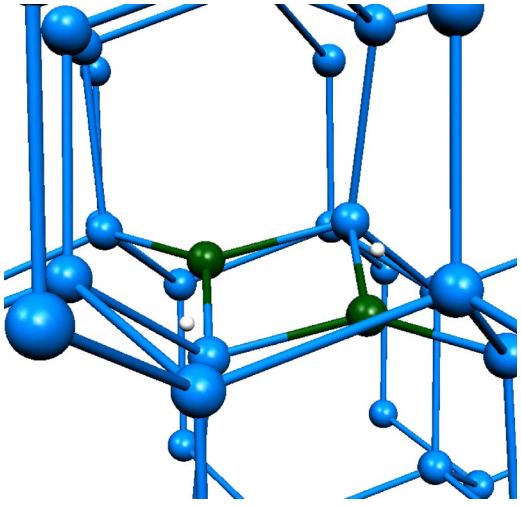

FIG. 5. (Color online) Fraction of the Si_{64} cell showing the $\{N_i,N_i\}$ complex. The light gray (blue) spheres are Si atoms, the darker gray (green) spheres are N atoms, and the small white balls show the substitutional sites.

of the three Si-N-Si bond angles is almost exactly 360°. This is a perfect trigonal planar structure, with N sp^2 hybridized. Its fourth and fifth valence electrons are in the $2p_z$ orbital, which points toward the fourth Si NN to the vacancy. This Si atom has a single electron in a dangling bond and we find it to be a trap for H (see below).

The dynamical matrix shows two local modes associated with the motion of the N atom: a doubly degenerate *E* mode (N-Si stretch) at 664 cm^{-1} and an A_1 mode at 222 cm^{-1}. The latter has N moving along the $\langle 111\rangle$ axis perpendicular to the plane defined by the N atom and its three Si NN's. The frequencies are compared to other predictions and experiment in Table II.

C. N_i-self-interstitial pair: $\{N_i,I\}$

If N_i encounters a *preexisting* Si self-interstitial I, it binds to it and the reaction $N_i+I\rightarrow\{N_i,I\}$ releases 1.73 eV. This complex (Fig. 4) has C_1 symmetry. Several host atoms are displaced from their perfect substitutional sites. N, I, and two Si NN's form an almost perfectly planar arrangement. In this quadrangle, the N-Si bond lengths are 1.6 and 1.79 Å, and the I-Si bond lengths are 2.38 and 2.36 Å. The bond angle between the N and its two Si NN's is 103°, the bond angle between I and the same two Si NN's is 72°, and the two I-Si-N bond angles are 93° each.

We identify seven vibrational modes with the $\{N_i,I\}$ complex. Three of them are associated with large oscillations of the N atom: 886 cm^{-1} (863 for ^{15}N) is the symmetric Si-N stretch, 765 cm^{-1} (746 for ^{15}N) is the antisymmetric Si-N stretch, and 255 cm^{-1} (251 for ^{15}N) has N moving in the $\langle 110\rangle$ direction, perpendicular to the plane defined by the N and its three NN's. The other modes involve large oscillations of I and its NN's: 542 cm^{-1} (540 for ^{15}N) is the breathing mode of the three Si's, 540 cm^{-1} (536 for ^{15}N) is the symmetric stretch of I and the neighboring Si, 147 cm^{-1} (147 for ^{15}N) is a wag mode, and 213 cm^{-1} (213 for ^{15}N) is the twisting mode of the quadrangle.

IV. NITROGEN PAIRS

A. Interstitial-interstitial pair: $\{N_i,N_i\}$

Four *a priori* possible $\{N_i,N_i\}$ dimers were considered, but only one was found to be stable. The interstitial N_2 molecule centered at the hexagonal interstitial site spontaneously dissociates. The interstitial N_2 molecule centered at the tetrahedral interstitial site and the structure proposed by Stein[2] (two N's at adjacent puckered BC sites) are 4.63 and 4.24 eV above the lowest-energy configuration, respectively. The stable structure of $\{N_i,N_i\}$ is the C_{2h} configuration proposed by Jones *et al.*[26] (Fig. 5). Each of the two N atoms is bound to three Si atoms and shares two of these. These two Si and the two N atoms form a square in the $\langle 110\rangle$ plane. The N atoms are separated by 2.47 Å. A population analysis shows that there is no covalent overlap between them.

A total of 12 modes are associated with $\{N_i,N_i\}$. The degrees of localization are shown in Fig. 6: both N atoms (top) and their two common Si NN's (bottom). The frequencies are compared to other predictions[43] and experiment[26] in Table III. Note that the pairs of modes at 531 cm^{-1} and at 263 cm^{-1} have distinct symmetries. Note also that the mode at 252 cm^{-1} exhibits an exceptionally strong localization. It corresponds to the two N atoms oscillating in opposite directions perpendicular to the plane of the square discussed above.

B. Interstitial-substitutional pair: $\{N_i,N_s\}$

The interactions of $\{N_i,N_i\}$ with a preexisting V or of N_i with N_s lead to the formation of the $\{N_i,N_s\}=\{N_2,V\}$ pair. The former reaction releases 1.42 eV and the latter 1.39 eV.

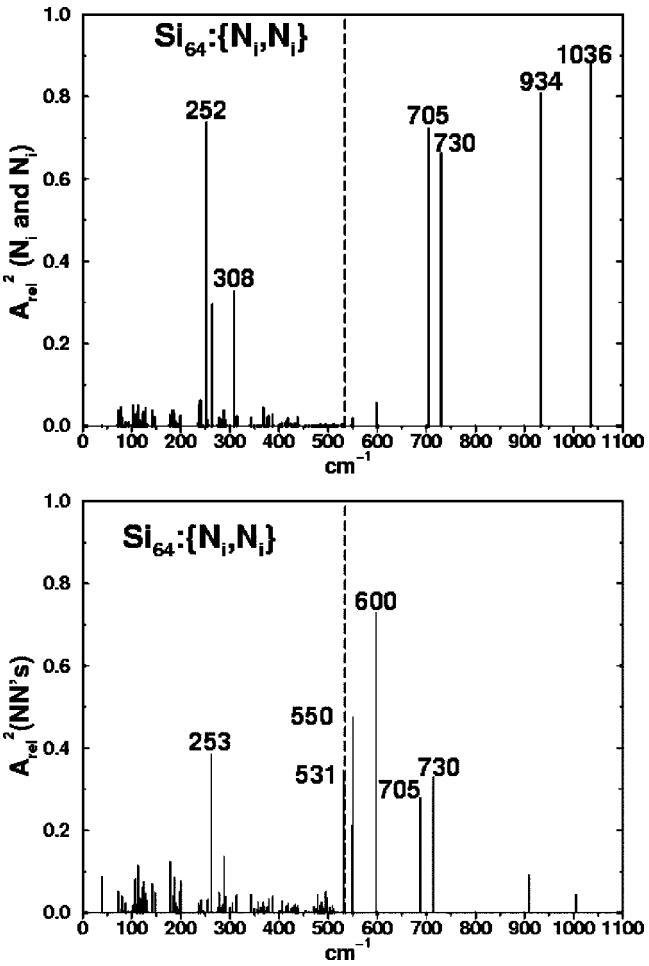

FIG. 6. Square amplitude of the oscillation of both N atoms in the $\{N_i,N_i\}$ complex (top) and both common Si NN's to the two N's (bottom), as a function of frequency. The dashed line shows the calculated Γ phonon.

TABLE III. Vibrational frequencies (cm^{-1}) associated with the $\{^{14}N_i,^{14}N_i\}$ complex in Si. The isotope substitutions are given in the Appendix.

C_{2h}	This work	Goss *et al.*[a]	Experiment[b]
A_g	1036	1070.0	
B_u	934	967.8	962.1
B_u	730	772.9	765.6
A_g	705	743.1	
A_g	600		
A_u	550		
B_u	531		
B_g	531		
A_u	308		
A_g	263		
A_u	263		
B_g	252		

[a]Reference 43.
[b]Reference 26.

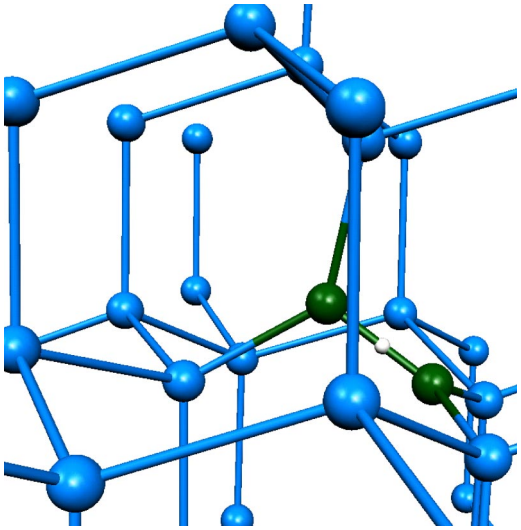

FIG. 7. (Color online) Fraction of the Si_{64} atom cell showing the $\{N_i,N_s\}$ defect. The light gray (blue) spheres are Si atoms, the darker gray (green) spheres are N atoms, and the small white ball shows the perfect substitutional site.

We placed a N_2 molecule at a vacancy site and performed a conjugate gradient optimization. The N-N bond lengthens from 1.10 Å (triple bond) to 1.46 Å (single bond), as each N binds to two dangling bonds of the vacancy. The two N's align along the $\langle 100\rangle$ axis (Fig. 7). The four N-Si bond lengths are 1.82 Å, the two Si-N-Si bond angles are 132°, and the four Si-N-N bond angles are 114°. The symmetry is D_{2d}.

Three LVM's and one pLVM associated with the oscillations of the two N atoms are listed in Table IV. One LVM and one pLVM due to the Si NN's are in Table IV. The mode at 875 cm^{-1} is the symmetric stretch of the two N_i's. The degenerate 773 cm^{-1} mode is the antisymmetric stretch of Si-N. The mode at 577 cm^{-1} is due to both N_i's moving in the same direction along the principal axis of the defect (a C_2 axis of the crystal). All four of the Si NN's moving symmetrically away from the substitutional site gives rise to the mode at 461 cm^{-1}. Finally, the degenerate 312 cm^{-1} is the N-Si wag mode.

C. Substitutional-substitutional pair: $\{N_s,N_s\}$

If V is a preexisting vacancy, the reaction $\{N_i,N_s\}+V \rightarrow \{N_s,N_s\}=\{N_2,V_2\}$ releases 4.06 eV (as compared to

TABLE IV. Vibrational frequencies (cm^{-1}) associated with the $\{^{14}N_i,^{14}N_s\}$ complex in Si. The isotope substitutions are given in the Appendix.

D_{2d}	This work	Goss *et al.*[a]
A_1	875	1004
E	773	774
B_2	577	573
A_1	461	
E	312	

[a]Reference 43.

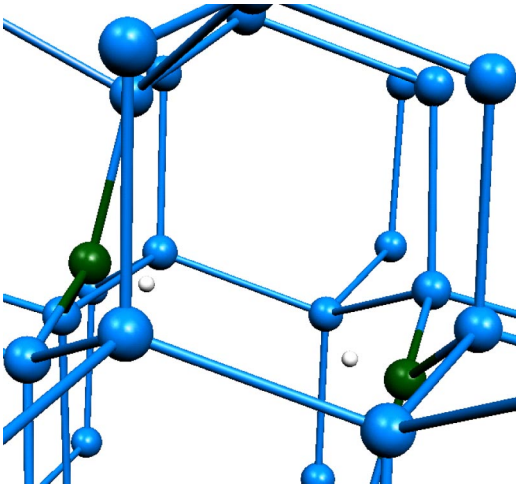

FIG. 8. (Color online) Fraction of the Si_{64} cell showing $\{N_s,N_s\}$. The light gray (blue) spheres are Si atoms, the darker gray (green) spheres are N atoms, and the small white balls show the perfect substitutional sites.

4.07 eV in Ref. 41 and 3.7 eV in Ref. 43). The $\{N_s,N_s\}$ complex (Fig. 8) resembles two adjacent N_s structures with zero overlap between the two N atoms. We find the N-N internuclear distance to be 3.68 Å, somewhat longer than other authors.[23,41,43] Each N is almost perfectly sp^2 hybridized and has a filled $2p_z$ orbital pointing toward the center of the divacancy. These orbitals repel each other. The symmetry is D_{3d}. Each of the six N-Si bond lengths is 1.84 Å. All six of the Si-N-Si bond angles are 119°.

Two LVM's and two pLVM's are listed in Table V. The degenerate 670 cm^{-1} mode is the symmetric N-Si stretch and the degenerate 663 cm^{-1} mode is the antisymmetric stretch. The lines at 320 and 284 cm^{-1} have the two N's moving perpendicular to the plane formed by N and its three Si NN's (similar to the 222 cm^{-1} mode of N_s): the N's are moving away from one another (320 cm^{-1}) or in the same direction (284 cm^{-1}).

V. NITROGEN-HYDROGEN COMPLEXES

The interactions between H and N_i, N_s and the $\{N_i,N_i\}$ pair have been studied. The $\{N_i,N_i\}$ pair is very stable and the N atoms are threefold coordinated with short N-Si bond lengths. This structure is unlikely to trap H

TABLE V. Vibrational frequencies (cm^{-1}) associated with the $\{N_s,N_s\}$ complex in Si. The isotope substitutions are given in the Appendix.

D_{3d}	This work	Goss *et al.*[a]
E_u	670	669
E_g	663	667
A_{1g}	320	
A_{2u}	284	

[a]Reference 43.

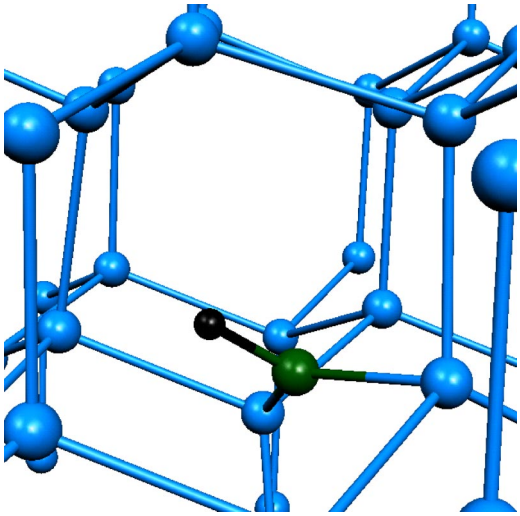

FIG. 9. (Color online) Fraction of the Si_{64} atom cell showing the lowest-energy configuration of the $\{N_i,H\}$ defect. The light gray (blue) spheres are Si atoms, the darker gray (green) sphere is N, and the small black sphere is H.

without generating additional strain. We find that the most stable $\{N_i,N_i,H\}$ complex has a binding energy of only 0.38 eV relative to isolated $\{N_i,N_i\}$ and H_{BC}. We will therefore focus on the $\{N_i,H\}$ and $\{N_s,H\}$ complexes only.

A. $\{N_i,H\}$

N_i is a strong trap for interstitial hydrogen. The reaction $N_i+H_{BC}\rightarrow\{N_i,H\}$ (where H_{BC} is isolated bond-centered hydrogen) releases 2.07 eV. We examined six *a priori* possible structures for the $\{N_i,H\}$ complex, starting with N_i (see Fig. 1): H antibonding to N, H antibonding to Si, H bridging one of the two equivalent N-Si bonds, H bridging

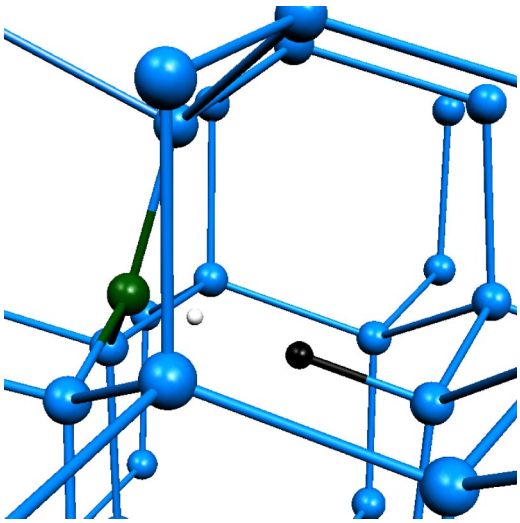

FIG. 10. (Color online) Fraction of the Si_{64} cell showing $\{N_s,H\}$. The light gray (blue) spheres are Si atoms, the darker gray (green) sphere is N, the small black sphere is H, and the white sphere shows the perfect substitutional site.

TABLE VI. Formation energies (eV) relative to the most stable defect $\{N_i,N_i\}$.

Defect	This work	Goss *et al.*[a]
$\{N_i,N_i\}$	0.00	0.00
$\{N_s,N_s\}$	0.86	0.79
$\{N_i,N_s\}$	1.09	0.99
$\{N_i\}$	1.76	1.83
$\{N_s\}$	1.81	1.99

[a]Reference 43.

the third N-Si bond, H bridging a Si-Si bond with one Si adjacent to N, and H at a tetrahedral or hexagonal interstitial site adjacent to N. The lowest-energy structure has N at a puckered BC site, with H bound to N (Fig. 9). The bond lengths are N-Si $=1.73$ Å (each) and N-H$=1.05$ Å. The Si-N-Si bond angle is 137°. This complex has C_1 symmetry.

There are four LVM's and three pLVM's associated with the $\{N_i,H\}$ complex. All the modes are IR active in C_1 symmetry. The N-H stretch is at 3065 cm^{-1} and the N-H wag is at 1160 cm^{-1}. The symmetric and antisymmetric N-Si stretch modes are at 992 and 638 cm^{-1}, respectively, and the antisymmetric N-H wag is at 319 cm^{-1}. Finally, two bending N-Si modes are at 205 and 182 cm^{-1}. The isotope substitutions are tabulated in the Appendix.

Pajot *et al.*[48] have reported a mode associated with an unspecified $\{N,H\}$ complex at 2967 cm^{-1} (2197 in deuterated samples). This is within 2–3 % of our calculated ^{14}N-H stretch mode of $\{N_i,H\}$ at 3065 cm^{-1} (2245 for ^{14}N-D, see the Appendix). On the other hand, the highest-lying LVM in the $\{N_s,H\}$ complex (see below) is the Si-H stretch at 2024 cm^{-1}, much lower in frequency. Therefore, the observed line is most likely associated with $\{N_i,H\}$.

B. $\{N_s,H\}$

The reaction $N_s+H_{BC}\rightarrow\{N_s,H\}$ releases 1.87 eV. Four structures were studied: H bonding or antibonding to the Si carrying the dangling bond, H antibonding to N, and H_{BC} between the Si with the dangling bond and an adjacent Si. Only one configuration is stable. It has H bound to the dangling Si bond (Fig. 10) in the bonding configuration. The symmetry is C_{3v}, the N-Si bond lengths are 1.85 Å, the Si-H bond length is 1.53 Å, and the separation between H and N is 1.90 Å.

The Si-H stretch (A_1 mode) is at 2024 cm^{-1}, the Si-N stretch (degenerate E mode) at 655 cm^{-1}, the Si-H wag (degenerate E mode) at 596 cm^{-1}, and the Si-N wag (A_1 mode) at 317 cm^{-1}. All these modes are IR active. The isotope substitutions are tabulated in the Appendix.

VI. DISCUSSION

First-principles DF-based MD simulations with local basis sets in 64 host-atom supercells are used to calculate the structures, energetics, and complete vibrational spectra of isolated N, $\{N,N\}$ pairs, and $\{N,H\}$ complexes in Si. The calculated properties of N_i, N_s, $\{N_i,N_i\}$, $\{N_i,N_s\}$, and $\{N_s,N_s\}$ agree quite well with the recent results of Goss *et al.*[43] except for the A_1 mode of $\{N_i,N_s\}$ which we find to be at 875 cm^{-1} but is given at 1004 cm^{-1} in Ref. 43. We also present here the theoretical predictions for the $\{N_i,I\}$ pair (I is the self-interstitial).

The formation energies of the various defects considered here are compared to those obtained in Ref. 43 in Table VI. The most stable complex is $\{N_i,N_i\}$. We reported above the binding energies of all the complexes relative to various dissociation products. In particular, we note that $\{N_i,N_i\}+V\rightarrow\{N_i,N_s\}+1.42$ eV (V is a preexisting vacancy) is a rather small binding energy as compared, for example, to V-V interactions.[65] On the other hand, the reaction $\{N_i,N_s\}+V\rightarrow\{N_s,N_s\}+4.06$ eV is much more energetic, and $\sim$4 eV is comparable to the vacancy formation energy.

We find a number of N-related modes, in particular, several rather strongly localized pLVM's which are calculated here. The pLVM's showing up in almost all N-related defects are in the 220–280 cm^{-1} range and correspond to Si-N wag modes. This is most pronounced in the case of the $\{N_i,N_i\}$ pair.

N_i and N_s are traps for hydrogen: $N_i+H_{BC}\rightarrow\{N_i,H\}+2.07$ eV and $N_s+H_{BC}\rightarrow\{N_s,H\}+1.87$ eV. These binding energies are smaller than those of H-vacancy defects. The $\{N_i,H\}$ and $\{N_s,H\}$ complexes have very different vibrational properties. In particular, $\{N_i,H\}$ has a N-H bond with a stretch frequency of 3065 cm^{-1}, while the highest-frequency mode of $\{N_s,H\}$ is a Si-H stretch at 2024 cm^{-1}. We assign the 2967 cm^{-1} line seen by Pajot *et al.*[48] to the $\{N_i,H\}$ pair. The $\{N_i,N_i\}$ complex is very stable and therefore at best a weak trap (0.38 eV) forhydrogen.

Of all the LVM's calculated here, only eight (including isotope substitutions) have been identified experimentally: Six for $\{N_i,N_i\}$ (Ref. 28) and two for N_s.[31] Our calculations agree to within $\sim$2–3 % for the higher-lying modes and $\sim$5% for the lower-frequency modes. Four more modes have been observed and attributed to N defects.

(a) The ^{14}N mode at 691 cm^{-1} (^{15}N mode at 674 cm^{-1}) has been tentatively assigned to N_i. These frequencies are close to our 725 cm^{-1} for $^{14}N_i$ (707 cm^{-1} for $^{15}N_i$). The experimental isotope shift is 17 cm^{-1}, compared to our calculated shift of 18 cm^{-1}.

(b) The 2967 cm^{-1} line (2197 in deuterated samples) was assigned to a $\{N,H\}$ complex. It is almost certainly the N-H stretch of the $\{N_i,H\}$ complex.

ACKNOWLEDGMENTS

This work was supported in part by a grant from the R. A. Welch Foundation and a contract from the National Renewable Energy Laboratory. Many thanks to Texas Tech's High Performance Computer Center for generous amounts of CPU time. H.R. was supported by the Clark Scholar Program during the summer of 2002.

APPENDIX: ISOTOPIC SUBSTITUTIONS

The following tables (Tables VII–XI) contain the vibrational frequencies for the isotope substitution not listed in the main text.

TABLE VII. Vibrational frequencies (cm^{-1}) for ^{15}N substitutions of $\{N_i,N_i\}$ complex (Table III).

Isotopes	Symmetry	This work	Experiment[a]
$^{15}N_i,^{15}N_i$	A_g	1005	
C_{2h}	B_u	909	936.3
	B_u	714	748.3
	A_g	688	
	A_g	598	
	A_u	550	
	B_u	531	
	B_g	531	
	A_u	305	
	A_g	262	
	A_u	260	
	B_g	247	
$^{14}N_i,^{15}N_i$	A'	1022	
C_{1h}	A'	919	946.9
	A'	725	758.5
	A'	694	
	A'	599	
	A''	550	
	A'	531	
	A''	531	
	A''	307	
	A'	262	
	A''	262	
	A''	249	

[a]Reference 26.

TABLE VIII. Vibrational frequencies (cm^{-1}) for ^{15}N substitutions of $\{N_i,N_s\}$ complex (Table IV). Note that the two nitrogen atoms are equivalent.

Isotopes	Symmetry	This work
$^{15}N_i,^{15}N_s$	A_1	846
D_{2d}	E	752
	B_2	568
	A_1	460
	E	309
$^{14}N_i,^{15}N_s$	A_1	861
C_{2v}	B_2	771
	B_1	753
	A_1	572
	A_1	461
	B_1	312
	B_2	310

TABLE IX. Vibrational frequencies (cm^{-1}) for ^{15}N substitutions of $\{N_s,N_s\}$ complex (Table V).

Isotopes	Symmetry	This work
$^{15}N_s,^{15}N_s$	E_u	652
D_{3d}	E_g	647
	A_{1g}	316
	A_{2u}	280
$^{14}N_s,^{15}N_s$	E	667
C_{3v}	E	649
	A_1	318
	A_2	282

TABLE X. Vibrational frequencies (cm^{-1}) for ^{15}N and D substitutions of $\{N_i,H\}$ complex. The symmetry is C_1.

Isotope	This work						
$^{14}N_i,H$	3065	1160	992	638	319	205	182
$^{14}N_i,D$	2245	1014	818	631	316	205	182
$^{15}N_i,H$	3058	1157	968	631	316	204	180
$^{15}N_i,D$	2236	1157	968	631	316	204	180

TABLE XI. Vibrational frequencies (cm^{-1}) for ^{15}N and D substitutions of $\{N_s,H\}$ complex. The symmetry is C_{3v}.

Isotope	A_1	E	E	A_1
$^{14}N_s,H$	2024	655	596	317
$^{14}N_s,D$	1436	648	515	315
$^{15}N_s,H$	1992	632	570	312
$^{15}N_s,D$	1436	632	515	311

*Electronic address: stefan.estreicher@ttu.edu.

[1] W. Kaiser and C.D. Thurmond, J. Appl. Phys. **30**, 427 (1959)
[2] H.J. Stein, in *Oxygen, Carbon, Hydrogen, and Nitrogen in Crystalline Silicon*, edited by J.C. Mikkelson, Jr., S.J. Peterson, J.W. Carbett, and S. J. Pennycook, Mater. Res. Soc. Symp. Proc. No. 59 (Materials Research Society, Pittsburgh, 1986), p. 523.
[3] K. Sumino, I. Yonenaga, M. Imai, and T. Abe, J. Appl. Phys. **54**, 5016 (1983)
[4] D. Li, D. Yang, and D. Que, Physica B **173-174**, 553 (1999).
[5] M.V. Mezhennyi, M.G. Milvidski, V. Ya Reznik, and R.J. Falster, J. Phys.: Condens. Matter **14**, 12 903 (2002).
[6] W.J.M.J. Josquin and Y. Tamminga, J. Electrochem. Soc. **129**, 1803 (1982).
[7] W.B. Knowlton, J.T. Walton, J.S. Lee, Y.K. Wong, E.E. Haller, W. von Ammon, and W. Zulehner, Mater. Sci. Forum **196-201**, 1761 (1995).
[8] M. Suezawa, K. Sumino, H. Harada, and T. Abe, Jpn. J. Appl. Phys., Part 1 **27**, 62 (1988).
[9] M.W. Qi, S.S. Tan, B. Zhu, P.X. Cai, F. Gu, X.M. Xu, T.S. Shi, D.L. Que, and L.B. Li, J. Appl. Phys. **69**, 3775 (1991)
[10] K. Nakai, Y. Inoue, H. Yokota, A. Ikari, J. Takahashi, A. Tachikawa, K. Kitahara, Y. Ohta, and W. Ohashi, J. Appl. Phys. **89**, 4301 (2001).
[11] X. Ma, X. Yu, R. Fan, and D. Yang, Appl. Phys. Lett. **81**, 496 (2002).
[12] J. Weber, W. Schmid, and R. Sauer, Phys. Rev. B **21**, 2401 (1980).
[13] H.Ch. Alt and L. Tapfer, Appl. Phys. Lett. **45**, 426 (1984).
[14] G. Davies, M. Zafar Iqbal, and E.C. Lightowlers, Phys. Rev. B **50**, 11 520 (1994).
[15] K. L Brower, Phys. Rev. Lett. **44**, 1627 (1980).
[16] K.L. Brower, Phys. Rev. B **26**, 6040 (1982).
[17] K. Murakami, H. Kuribayashi, and K. Masuda, Phys. Rev. B **38**, 1589 (1988).
[18] J.A. Vergés, J. Phys. C **14**, 365 (1981).
[19] G.D. Watkins, G.G. DeLeo, and W.B. Fowler, Physica B & C **116**, 28 (1983); G.G. DeLeo, W.B. Fowler, and G.D. Watkins, Phys. Rev. B **29**, 3193 (1984).
[20] R.P. Messmer and P.A. Schultz, Solid State Commun. **52**, 563 (1984); Phys. Rev. B **34**, 2532 (1986).
[21] H.P. Hjalmarson and D.R. Jennison, Phys. Rev. B **31**, 1208 (1985).
[22] F.G. Anderson, Phys. Rev. B **39**, 5392 (1989).
[23] C. Cunha, S. Canuto, and A. Fazzio, Phys. Rev. B **48**, 17 806 (1993).
[24] M. Saito and Y. Miyamoto, Phys. Rev. B **56**, 9193 (1997).
[25] J.B. Mitchell, P.P. Pronko, J. Shewchun, D.A. Thompson, and J.A. Davies, J. Appl. Phys. **46**, 332 (1975).
[26] R. Jones, S. Öberg, F. Berg Rasmussen, and B. Bech Nielsen, Phys. Rev. Lett. **72**, 1882 (1994).
[27] J.B. Mitchell, J. Shewchun, D.A. Thompson, and J.A. Davies, J. Appl. Phys. **46**, 335 (1975).
[28] H. J. Stein, in *Proceedings of the 13th International Conference on Defects Semiconductors*, edited by L. C. Kimerling and J. M. Parsey, Jr. (Metallurgical Society of AIME, Warrendale, PA, 1985), p. 839.
[29] H.J. Stein, P.S. Peercy, and C.R. Hills, in *Energy Beam-Solid Interactions and Transient Thermal Processing*, edited by D. K. Biegelsen, G. A. Rozgonyi, and C. V. Shank, Mater. Res. Soc. Symp. Proc. No. 35 (Materials Research Society, Pittsburgh, 1985), p. 315.
[30] H.J. Stein, in *Microscopic Identification of Electronic Defects in Semiconductors*, edited by N.M. Johnson, S.G. Bishop, and G. D. Watkins, Mater. Res. Soc. Symp. Proc. No. 46 (Materials Research Society, Pittsburgh, 1985), p. 839.
[31] H.J. Stein, Appl. Phys. Lett. **47**, 1339 (1985)
[32] H.J. Stein, Appl. Phys. Lett. **52**, 153 (1988).
[33] B. Bech Nielsen (private communication).
[34] F. Berg Rasmussen, R. Jones, and S. Öberg, Phys. Rev. B **50**, 4378 (1994).
[35] P.A. Schultz and J.S. Nelson, Appl. Phys. Lett. **78**, 736 (2001).
[36] H. Sawada, K. Kawakami, A. Ikari, and W. Ohashi, Phys. Rev. B **65**, 075201 (2002).
[37] H. Ishii, S. Shiratake, K. Oka, K. Motonami, T. Koyama, and J. Izumitani, Jpn. J. Appl. Phys., Part 2 **35**, L1385 (1996).
[38] L.S. Adam, M.E. Law, S. Szpala, P.J. Simpson, D. Lawther, O. Documaci, and S. Hegde, Appl. Phys. Lett. **79**, 623 (2001).
[39] W. von Ammon, R. Hölzl, J. Virbulis, E. Dornberger, R. Schmolke, and D. Gräf, J. Cryst. Growth **226**, 19 (2001); Solid State Phenom. **82-84**, 17 (2002).
[40] H. Sawada and K. Kawakami, Phys. Rev. B **62**, 1851 (2000).
[41] H. Kageshima, A. Taguchi, and K. Wada, Appl. Phys. Lett. **76**, 3718 (2000).
[42] H. Harada, I. Ohkubo, T. Mikayama, Y. Yamanaka, and N. Inoue, Physica B **308-310**, 244 (2001).
[43] J.P. Goss, I. Hahn, R. Jones, P.R. Briddon, and S. Öberg, Phys. Rev. B **67**, 045206 (2003).
[44] S.K. Estreicher, Mater. Sci. Eng., R. **14**, 319 (1995).
[45] S.J. Pearton, J.W. Corbett, and M.J. Stavola, *Hydrogen in Crystalline Semiconductors* (Springer-Verlag, Berlin, 1992).
[46] A. Rohatgi, P. Doshi, J. Moschner, T. Lauinger, A.G. Aberle, and D.S. Ruby, IEEE Trans. Electron Devices **47**, 987 (2000).
[47] C. Boehme and G. Lukovski, J. Appl. Phys. **88**, 6055 (2000); J. Vac. Sci. Technol. A **19**, 2622 (2001).
[48] B. Pajot, B. Clerjaud, and Z.-J. Xu, Phys. Rev. B **59**, 7500 (1999).
[49] S.K. Estreicher, D. West, J. Goss, S. Knack, and J. Weber, Phys. Rev. Lett. **90**, 035504 (2003).
[50] D. Sánchez-Portal, P. Ordejón, E. Artacho, and J.M. Soler, Int. J. Quantum Chem. **65**, 453 (1997).
[51] E. Artacho, D. Sánchez-Portal, P. Ordejón, A. García, and J.M. Soler, Phys. Status Solidi B **215**, 809 (1999).
[52] D.M. Ceperley and B.J. Alder, Phys. Rev. Lett. **45**, 566 (1980).
[53] S. Perdew and A. Zunger, Phys. Rev. B **23**, 5048 (1981).
[54] L. Kleinman and D.M. Bylander, Phys. Rev. Lett. **48**, 1425 (1982).
[55] O.F. Sankey and D.J. Niklevski, Phys. Rev. B **40**, 3979 (1989); O.F. Sankey, D.J. Niklevski, D.A. Drabold, and J.D. Dow, *ibid.* **41**, 12 750 (1990).
[56] A.A. Demkov, J. Ortega, O.F. Sankey, and M.P. Grumbach, Phys. Rev. B **52**, 1618 (1995).
[57] H.J. Monkhorst and J.D. Pack, Phys. Rev. B **13**, 5188 (1976).
[58] J.M. Pruneda, S.K. Estreicher, J. Junquera, J. Ferrer, and P. Ordejón, Phys. Rev. B **65**, 075210 (2002).
[59] *Handbook of Chemistry and Physics*, 72nd ed., edited by D.R. Lide (CRC Press, Boston, MA, 1991).
[60] T. Shimanouchi, in *Tables of Molecular Vibrational Frequencies*

Consolidated Volume I, data from NIST Standard Reference Database 69–July 2001 Release: NIST Chemistry WebBook, edited by P. J. Linstrom and W. G. Mallard (NIST, 2001).
[61] W.D. Allen and H.F. Schaefer III, Chem. Phys. **108**, 243 (1986).
[62] D.B. Beach, Inorg. Chem. **31**, 4174 (1992).
[63] See, e.g., J.L. Hastings, S.K. Estreicher, and P.A. Fedders, Phys. Rev. B **56**, 10 215 (1997).
[64] H. Sawada and K. Kawakami, Appl. Phys. Lett. **76**, 3718 (2000).
[65] S.K. Estreicher, J.L. Hastings, and P.A. Fedders, Appl. Phys. Lett. **70**, 432 (1997).